

APPLICATIONS OF MOTORIZED ROTATIONAL RFEC PROBES IN THICK AND MULTILAYER STRUCTURE CRACK DETECTION

Y. Sun, W. Wan, X. Yang, C. Sun, H. Zhu and T. Ouyang

Innovative Materials Testing Technologies, Inc.
3141 W. Torreys Peak Drive, Superior, CO 80027

ABSTRACT. Crack detection in thick and multilayer structures has been a challenge to NDI/NDE societies. Remote field eddy current probes have shown features in deep penetration and high sensitivity. Motorizing the probes is an approach to improve the consistency of the signal received from the probe that enables on-the-spot signal processing and crack identification. It also minimizes human factor in crack detection. The newly developed NDI/NDE system provides higher reliability, repeatability, and confidence in crack detection in thick and multilayer structures.

Keywords: crack detection, thick and multilayer structure, remote field eddy current, motorization of probe rotation, on-the-spot signal processing, on-the-spot crack identification, reliability.

PACS: 8170.Ex, 81.40.Np

INTRODUCTION

To detect a small crack in a multilayer structure with a total thickness of 0.5” – 0.6” without fastener removal is a demand to NDI societies and a challenge to any existing or emerging NDI techniques. Examples include:

1. Ultrasonic techniques (UT), including guided UT, are incapable of penetrating through air gaps between two adjacent layers without sealant, or with aging sealant with possible disbond or cracking.
2. X-ray techniques, involving heavy equipment protecting operators from radiation, is relatively expensive, and has difficulty reliably detecting small cracks.
3. Most eddy current techniques (ECT) including conventional eddy current technique, eddy current array, magneto-optical imaging (MOI), and MWM, etc. have inherent limitation in penetration depth from their working principle – the Skin Depth.
4. In some eddy current and transit eddy current techniques, including these emerging techniques, magnetic sensors, such as Hall element, MR, GMR, etc., are used to replace coil sensor. Coil sensor has lower sensitivity at lower frequencies due to its induction working principle, because the signal is directly proportional to the excitation frequency. Higher sensitivity is expected at low frequencies with the use

of the magnetic sensors, because their working principle is direct measurement of magnetic field which is independent of the excitation frequency.

However, there is another barrier for detection of deep flaw signals that is how to separate a weak electromagnetic (EM) signal generated by a deeply hidden flaw (secondary signal) from the strong signal generated by the excitation coil (primary signal). A number of different approaches are used for the separation in different techniques, such as compensation and cancellation of the primary signal using reference primary signal obtained before or after the detection; magnetically shielding the sensor from the primary signal, etc.

These approaches of the signal separation may work well when the secondary signal is greater than a certain percentage of the primary signal, such as 1% - 0.1%, which we see in most surface and subsurface crack detection. However, in detection of a small crack located below 0.250" – 0.60" thick aluminum structure, the secondary/primary signal ratio can be drop to 0.001% - 0.0001%. The currently used signal separation approaches are no longer effective.

Among all ECT's, the Flat-Geometry Remote Field Eddy Current (FG_RFEC) probe is the only one that its penetration depth is not limited by Skin-Depth, because the signal received by its receiving unit has penetrated through the object wall twice. The measured signal is independent, or has minimum interference, from the primary signal. It carries clean, from the contamination of the excitation signal, information about the wall conditions.

Advanced signal processing and pattern recognition are often needed for crack detection in thick and multilayer. Unlike surface and subsurface crack detection, in detection of deeply hidden cracks signal magnitude may not necessarily be an indication of the existence of a crack. Other parameters, such as phase angle, the shape of the measured impedance plane, etc. will be used for crack identification and quantification. Furthermore, background noise, caused by structure and material variations, such as a layer edge close to the fastener; variation of thickness of any of the structure layers close to the fastener, fastener material and material property (conductivity and permeability) variation, etc. may consist of a major component of the detected signal. Advanced signal processing algorithms and even pattern recognition methods are badly needed in the crack identification and quantification. These functions should be built-in to the instrument. The computerized Super Sensitive Eddy Current (SSEC) instrument has shown good capability in this area.

FG_RFEC & SSEC TECHNIQUE AND ROTATIONAL PROBE

The original Remote Field Eddy Current (RFEC) technique has been used in NDI of conducting tubing for years. The RFEC technique is characterized by its features of deep penetration and the linear relation of its signal-phase to the total wall-thickness under inspection. The signal-phase to wall-thickness relation is independent of probe lift-off and the location of a flaw with respect to the wall thickness.

IMTT has expanded the applications of RFEC techniques to the inspections of conducting objects of flat or nearly flat geometries with the help of specially designed probes, called FG RFEC probes, and instrument, called SSEC instrument [1].

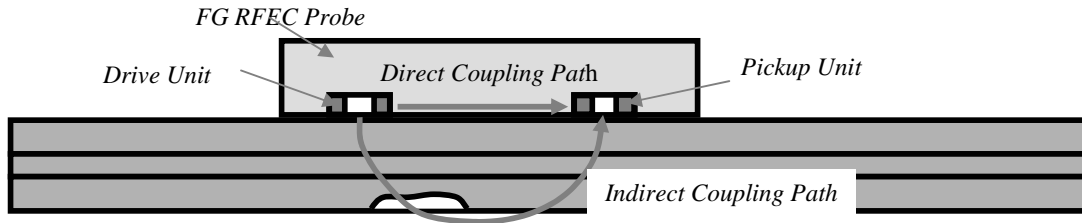


FIGURE 1. Simplified drawing of an FG RFEC probe and the energy coupling paths.

This technique consists of two major components: FG RFEC probe/technique and SSEC instrument.

There are at least two units, drive unit and pickup unit, in an FG RFEC probe, see Fig. 1. The probe is designed in a way that the two units are magnetically isolated. Therefore, there is no direct coupling between the two units. The electromagnetic energy released from the drive unit reaches the pickup unit through the indirect coupling path. Thus the signal received by the pickup unit carries the entire information about the wall thickness. The signal is very weak, but very clean, because it has no interference from the powerful drive signal.

The pickup signal is then sent to the second component, the SSEC instrument.

An SSEC instrument is a modified version of a conventional eddy-scope. An SSEC instrument has comparatively high gain and low noise level. It brings the weak pickup signal to a level that is readable on a computer screen. SSEC has built-in functions for automatic drive and control for scanners, on – the – spot signal processing, crack identification and quantification, etc. Furthermore, it accepts customized functions on signal processing and pattern recognition algorithms.

Current version of an SSEC instrument consists of a piece of software and two Printed Circuit Boards (PCBs) that are installed in a small box and can be connected to a customer-preferred computer or laptop through a universal serial port (USB), see Fig. 2.

The traditionally used raster scan or C-scan, using a sliding probe, has a disadvantage that the lower-layer crack signals are often submerged by the fastener signals/noises that may be hundreds times greater than the crack signals. For accurate and fast detection of fastener-hole cracks a series of rotational FG_RFEC probes have been developed. A rotational probe may minimize the noises if the probe is rotating right at the fastener center because of the geometric symmetry, Fig. 3. The rotational FG_RFEC probes have been applied to a number of different aircraft inspection applications. Examples include crack detection of C-130 lower wing splice structure and F-18 front spar structure [2, 3 and 4].



FIGURE 2. Photo of an SSEC instrument box AND system.

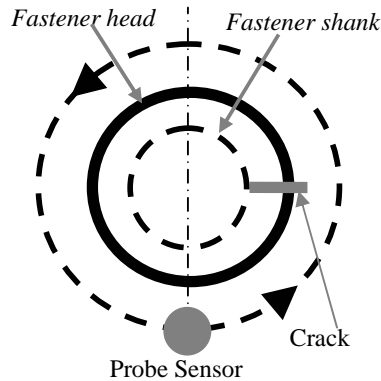


FIGURE 3. Minimizing noise from a fastener by rotating a probe around the fastener.

MOTORIZATION OF PROBE ROTATION

For identification and quantification of deeply hidden cracks the utilization of advanced signal processing and pattern recognition becomes essential. High repeatability of probe signals is required when advanced signal processing or/and pattern recognition algorithms are applied to the signal data. Motorization of probe rotation can provide a controlled constant rotation speed of rotational probe, thus ensures highly repeatable signal. The photo shown in Fig. 4 is a typical motorized FG-RFEC probe with a built-in motor controller. The motorized probe is fully driven and controlled by an SSEC II instrument.

The entire process of motor control, probe centering, signal-processing, crack identification and quantification has been automated using a number of pieces of software built-in to the SSEC instrument.

ADVANCE PERFORMANCES OF MOTORIZED FG_RFEC PROBE

Detecting vertically aligned cracks in a representative Boeing 707 wing structure is used as an example. A simplified drawing of the structure is shown in Fig. 5. This is a 0.250" + 0.310" thick two-layer structure made of aluminum alloy. Cracks were in second layer representative stringer structure below wing skins. All cracks were corner cracks of different sizes and shapes representing a crack growing from a 0.100" corner crack to a thru crack. There are four cases consisting of two fastener materials, titanium and steel, and two fastener rows with different crack-edge locations.

The best record of all current NDI techniques shows that in this particular applications the smallest detectable second layer crack is about 0.250" in length.

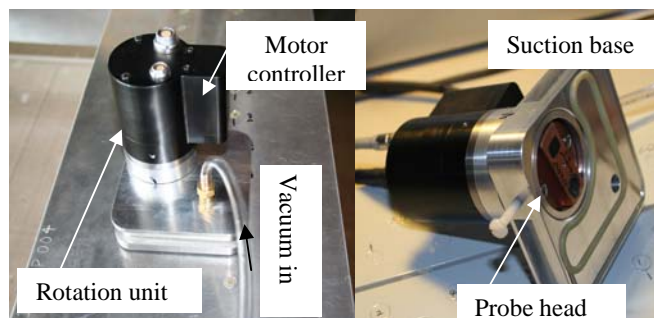


FIGURE 4. A typical motorized FG_RFEC rotational probe.

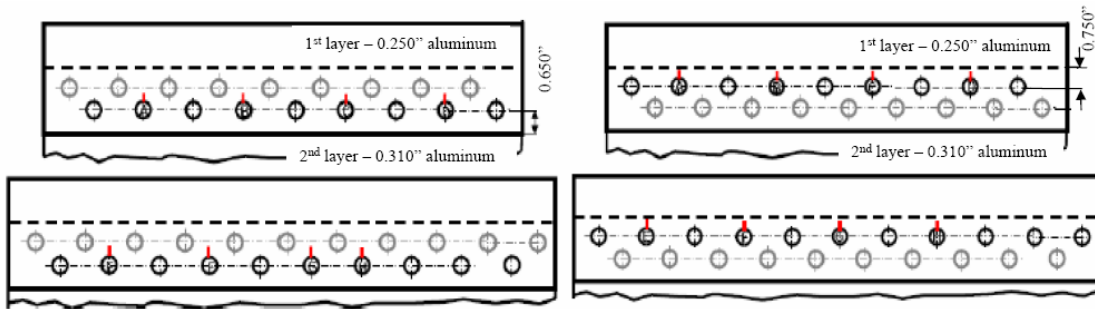


Figure 5. A representative Boeing 707 wing structure, inner row (left) and outer row (right) fasteners

Case No. 1 – Ti fastener and inner row

The special point in this case is that there is a close edge of the first layer which is about 0.650” away from the fastener center. The cracks are on the other side of the fasteners.

The original signals measured, using a motorized FG_RFEC probe, from no-crack and crack fasteners are shown in Figure 6. We see no visible difference between signal magnitudes of the two-kind signals: with crack and without crack. Signal process looks absolutely necessary for the crack identification and quantification.

If we carefully compare these impedance planes, we see rotation of the impedance patterns with increase of crack size. In order to quantify the rotation of the impedance patterns a curve fitting algorithm is applied to the impedance planes.

The test and internal signal processing procedure is as follows:

1. Center the probe rotation on no-crack fasteners and record the impedance planes of the measures signals.
2. Do curve fitting on theses signals using ellipses.
3. Change the SSEC rotation angle setting to have the averaged angle of the major axes of these ellipses to be zero, as shown in Fig. 7.

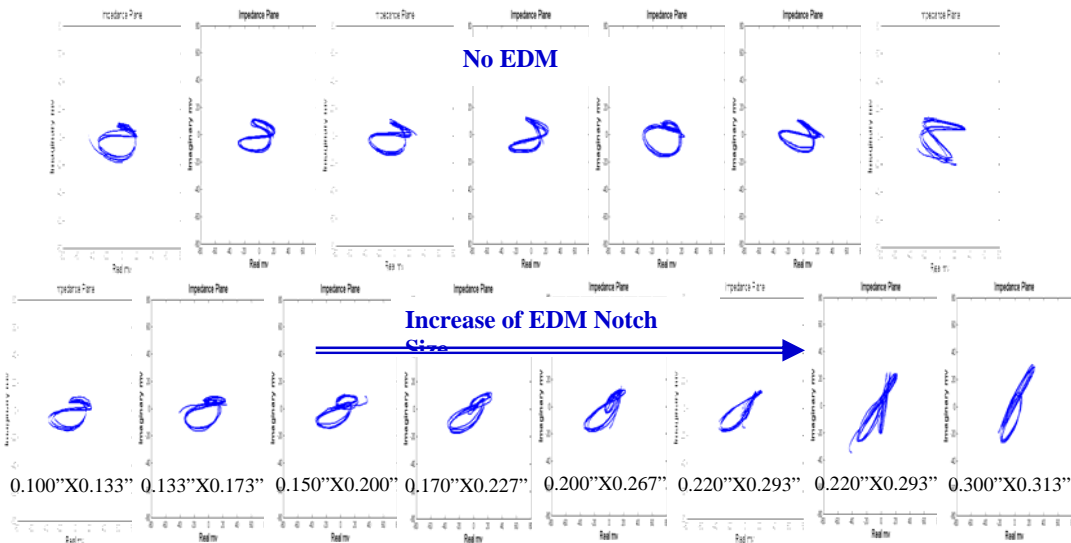


Figure 6. A original impedance planes from no-crack and crack fasteners for Case No. 1

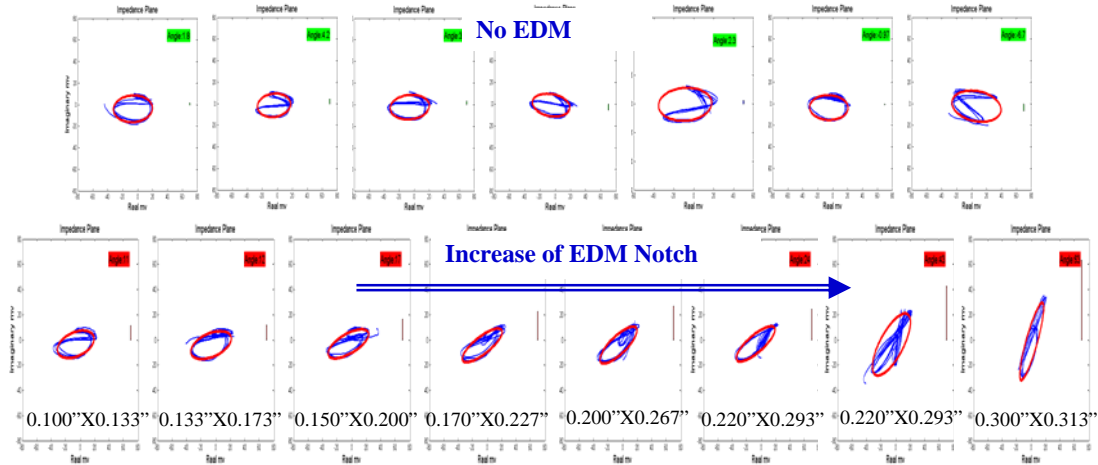


Figure 7. Ellipse curve fitting on the impedance planes for Case No. 1.

4. Center the probe rotation on fasteners with cracks in their holes and measure their impedance planes. Do curve fitting on these signals, as shown in Fig. 7.
5. Calculate the angle of the major axis of each of the signals. The major axis angle can be used as the indication of existence of a crack, also a measure of the crack size.
6. Plot out the angle variation as a function of crack size, as shown in Fig. 8.

With the help of the curve fitting algorithm and the test results shown in Fig. 8 it is confident to say that all the cracks in Case No. 1 are detected. The smallest is $.100'' \times .133''$.

Case No. 2 – Ti fastener and outer row

The special point in this case is that there is a close edge of the second layer which is about 0.750'' away from the titanium fastener center. A potential challenge in this case is the second layer edge and the cracks are on the same side of the fasteners.

Same test procedure and algorithm is applied to Case No.2. The final results are shown in Fig. 9. The smallest detectable crack is $0.133'' \times .173''$.

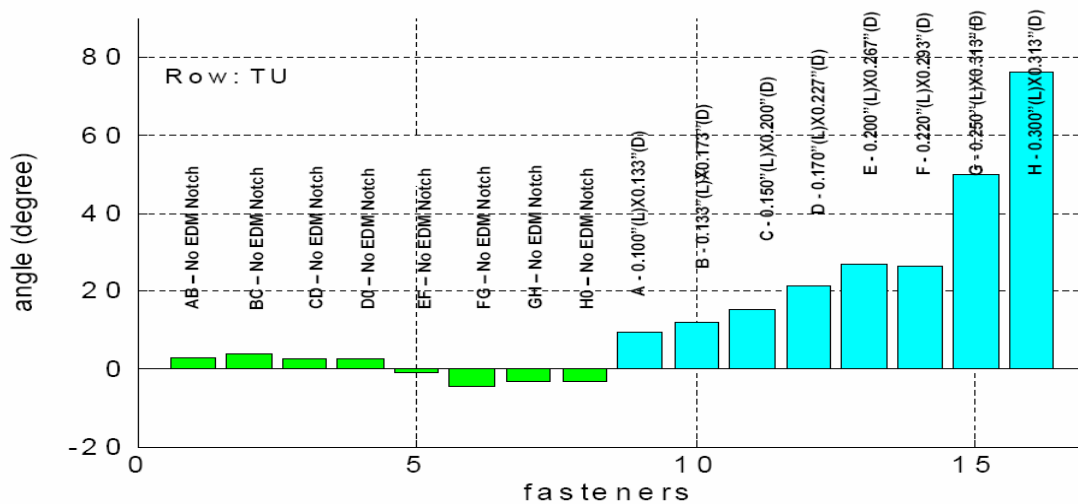


Figure 8. Diagram showing the ellipse major axis angle variation with crack size for Case No. 1.

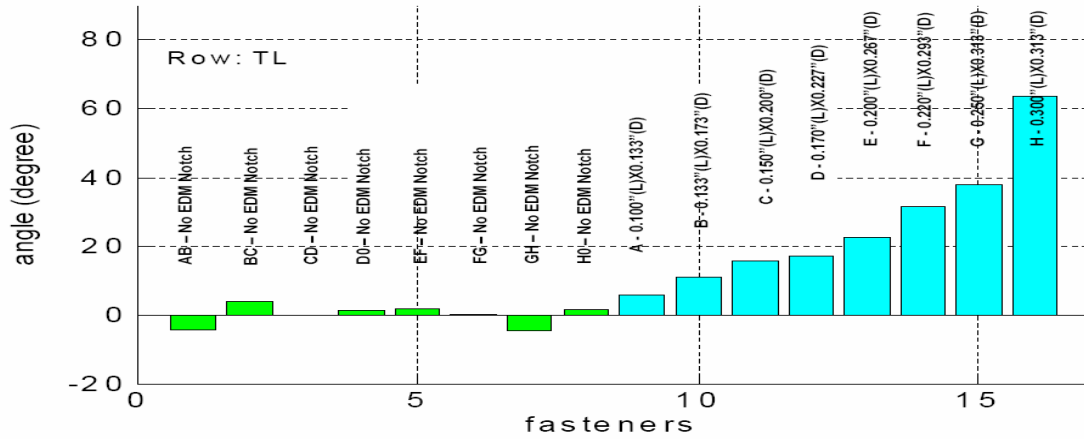


Figure 9. Diagram showing the ellipse major axis angle variation with crack size for Case No. 2.

Case No. 3 – Fe fastener and inner row

This case is almost identical to Case No. 1, but the fastener material is steel. Same procedure and algorithm is applied to this row of fasteners. The final results are shown in Fig. 10. The smallest detectable crack for Case No. 3 is .150”x.200”.

Case No. 4 – Fe fastener and outer row

The special point in this case is that there is a close edge of the second layer which is about 0.750” away from the steel fastener center. The real challenge is that the second layer crack and the second layer edge are on the same side of the steel fasteners.

Unlike the Case No. 2, where the second layer edge and cracks are on the same side of a titanium fastener, in Case No. 4 the fastener is made of steel. In this particular case crack signal DECREASES with increase of notch size as shown in Fig. 11. The underline physics of this phenomenon so far remains unknown.

A simple angle of impedance pattern rotation is no long working in this case for crack identification. A special Shape Factor P, which is a function of a few features of the impedance pattern, is used to represent the existence and size of a crack. The Factor P variation as a function of crack size is shown in Fig. 12. It is seen the smallest detectable crack is 0.150” x .200” if it requires S/N ≥ 2.5, or 0.200”x.267” if S/N ≥ 3.0.

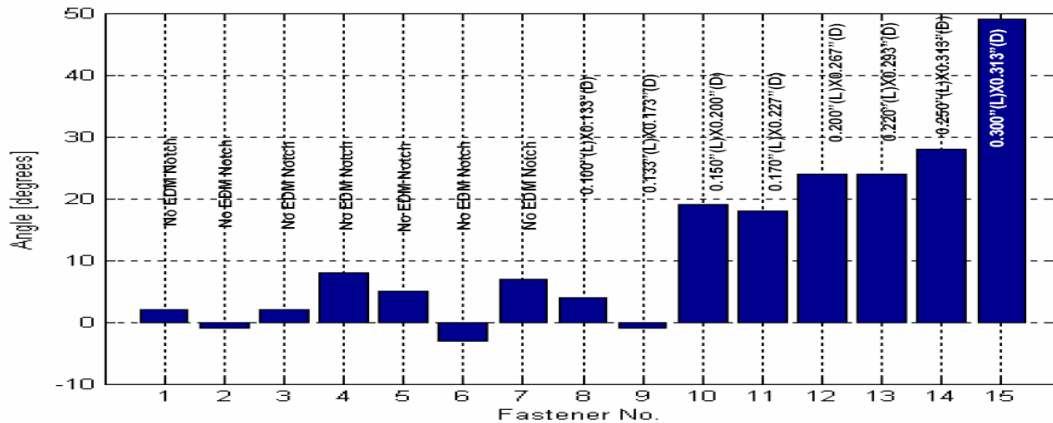


Figure 10. Diagram showing the ellipse major axis angle variation with crack size for Case No. 3.

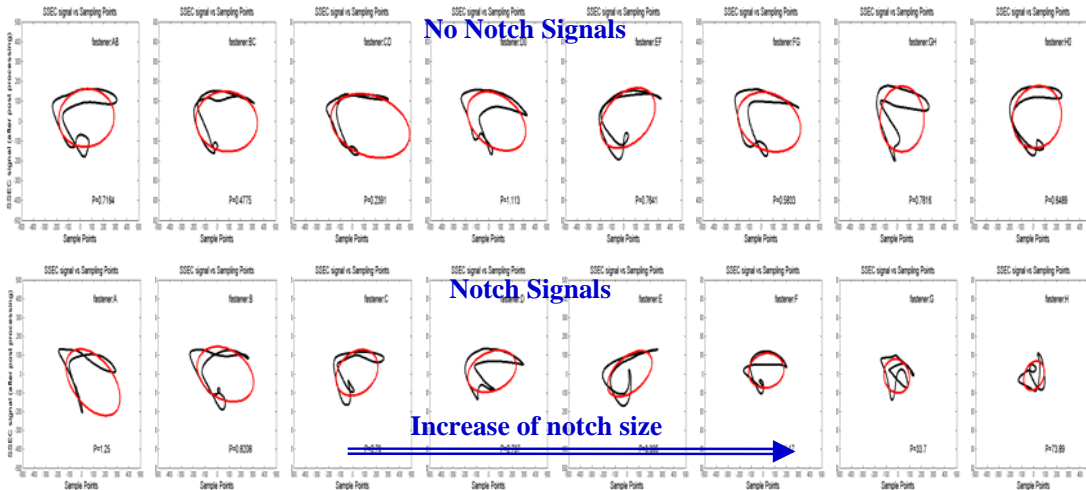


Figure 11. Impedance planes and ellipse curve fitting on the impedance planes for Case No. 4.

CONCLUSION

Motorization of rotational FG_RFEC probe enables on-the-spot signal processing and crack identification, thus enhances the capability of detecting small cracks in thick and multilayer structures.

REFERENCES

1. Y.S. Sun, T. Ouyang and S Udpa, *Materials Evaluation*, Volume 59/Number 5, May 2001.
2. Yushi Sun, John C. Brausch, Kenneth J. LaCivita, Lt William Sanders, , *Proceedings of The 9th FAA/DoD/NASA Joint Conference on Aging Aircraft*, presented on March 8, 2006, Session 27, the third presentation and paper, Atlanta, GA, March 6-9, 2006.
3. Yushi Sun, Tianhe Ouyang, and Robert J. Lord, *Proceedings of The 5th FAA/DoD/NASA Joint Conference on Aging Aircraft, PS28.pdf*, Kissimmee, Florida, September 10~13, 2001.
4. D.J. Butcher and Yushi Sun, *Proceedings of 2006 ASIP Conference*, presented at 10:00 AM – 10:30 AM, Wednesday, November 29, 2006, San Antonio, TX, November 27-30, 2006.

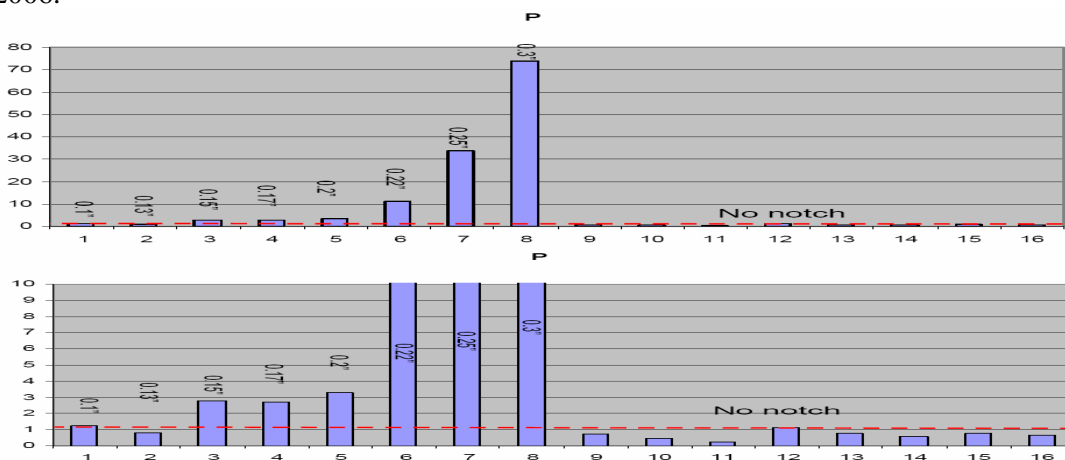


Figure 12. Diagram showing the variation of Shape-Factor P with crack size for Case No. 4. Upper – original; lower – zoom-in.